Biotechnol Lett (2012) 34:831–838
DOI 10.1007/s10529-011-0845-8

ORIGINAL RESEARCH PAPER

Flavonoid-mediated inhibition of SARS coronavirus 3C-like protease expressed in *Pichia pastoris*

Thi Thanh Hanh Nguyen · Hye-Jin Woo · Hee-Kyoung Kang · Van Dao Nguyen · Young-Min Kim · Do-Won Kim · Sul-Ah Ahn · Yongmei Xia · Doman Kim

Received: 24 October 2011 / Accepted: 22 December 2011 / Published online: 15 February 2012

Abstract The 3C-like protease ($3CL^{pro}$) of severe acute respiratory syndrome associated coronavirus (SARS-CoV) is vital for SARS-CoV replication and is a promising drug target. Recombinant $3CL^{pro}$ was expressed in *Pichia pastoris* GS115 as a 42 kDa protein that displayed a K_m of 15 ± 2 μM with Dabcyl-KTSAVLQSGFRKME-Edans as substrate. Purified $3CL^{pro}$ was used for inhibition and kinetic assays with seven flavonoid compounds. The IC_{50} of six flavonoid compounds were 47–381 μM. Quercetin, epigallocatechin gallate and gallocatechin gallate (GCG) displayed good inhibition toward $3CL^{pro}$ with IC_{50} values of 73, 73 and 47 μM, respectively. GCG showed a competitive inhibition pattern with K_i value of 25 ± 1.7 μM. In molecular docking experiments, GCG displayed a binding energy of -14 kcal mol^{-1} to the active site of $3CL^{pro}$ and the galloyl moiety at 3-OH position was required for $3CL^{pro}$ inhibition activity.

Keywords Flavonoid · Molecular docking · *Pichia pastoris* · Protease · Severe acute respiratory syndrome (SARS)

Electronic supplementary material The online version of this article (doi:10.1007/s10529-011-0845-8) contains supplementary material, which is available to authorized users.

T. T. H. Nguyen · H.-J. Woo · H.-K. Kang · D. Kim (✉)
School of Biological Sciences and Technology and the Research Institute for Catalysis, Chonnam National University, 77 Yongbong-ro, Buk-gu, Gwangju 500-757, Republic of Korea
e-mail: dmkim@jnu.ac.kr

T. T. H. Nguyen · H.-J. Woo · H.-K. Kang · D. Kim
Department of Pediatrics, University of California, San Diego, CA 92103, USA

V. D. Nguyen
Biotechnology Faculty, Hanoi Open University, 46 Ta Quang Buu street, Hai Ba Trung District, Hanoi, Vietnam

Y.-M. Kim
Eco-Friendly Biomaterial Research Center, Korea Research Institute of Bioscience and Biotechnology, Jeongeup 580-185, Republic of Korea

D.-W. Kim
Department of Physics, Gangeung-wonju National University, Gangneung 210-702, Republic of Korea

S.-A. Ahn
Global Science Experimental Data Hub Center, Korea Institute of Science and Technology Information, Daejeon 805-306, Republic of Korea

Y. Xia
State Key Laboratory of Food Science and Technology, Jiangnan University, 214122 Jiangsu, China

Introduction

In 2002, the first reported outbreak of severe acute respiratory syndrome (SARS) occurred in Guangdong province, China. It rapidly spread to over 32 countries in Asia, North America, and Europe. The mortality rate was approximately 10%, according to World Health Organization data. The causative agent of SARS is a novel human coronavirus (CoV), designated SARS-CoV. An efficient therapy and a vaccine are not currently available (Xu et al. 2005). SARS-CoV is an enveloped positive single-stranded RNA virus (Rota et al. 2003) that encodes two proteases for proteolytic processing: a papain-like cysteine protease ($PLP2^{pro}$) and a chymotrypsin-like cysteine protease (3C-like protease; $3CL^{pro}$) located in the non-structural protein regions nsp3 and nsp5, respectively. Since $3CL^{pro}$ is essential for the viral life cycle, it is an attractive target for the development of antiviral drugs directed against SARS-CoV and other CoV infections (Grum-Tokars et al. 2008).

Flavonoids are a large group of naturally occurring phenolic compounds ubiquitously distributed in the plant kingdom. Over 4,000 varieties of flavonoids have been identified (de Groot and Rauen 1998). Flavonoids can act as potent antioxidants, and display anti-inflammatory, antiallergic, antihemorrhagic, antimutagenic, antineoplastic, and hepatoprotective activities (Tapas et al. 2008; de Groot and Rauen 1998). In addition, flavonoids inhibit the catalytic activities of a great variety of enzymes, including hexokinase, phospholipase C, protein kinase C, α-glucosidase, and α-amylase. (Tadera et al. 2006). Some flavonoid compounds such as quercetin, quercetin derivatives, catechin, epicatechin, epicatechin gallate and epigallocatechin gallate inhibit SARS-$3CL^{pro}$ expressed in *Escherichia coli* (Chen et al. 2005, 2006; Yi et al. 2004). However, there has been no report on the high inhibition activity of gallocatechin gallate (GCG) against SARS-$3CL^{pro}$, or the structure–activity relationship activity among the aforementioned flavonoid compounds.

Herein, we report on the expression of SARS-$3CL^{pro}$ in *Pichia pastoris* GS115, its' in vitro inhibition by seven flavonoid compounds belonging to four groups of flavonoids (flavonol, flavanonol, isoflavone, and flavan-3-ol), and the structure–activity relationship between them. The detailed mechanism of GCG inhibition was investigated by enzyme kinetic and molecular docking studies.

Materials and methods

Preparation of recombinant $3CL^{pro}$

The procedures for construction, transformation, and screening for the catalytic domain of SARS $3CL^{pro}$ were according to the manufacturer's instructions (Invitrogen, Carlsbad, CA, USA). The gene encoding SARS $3CL^{pro}$ polyprotein (amino acid residues 3,241–3,546, GenBank accession no. AY274119) (Benson et al. 2011) was optimized by replacing rare codons with high-frequency codons, which were selected on the basis of the findings for codons usage in *Pichia pastoris* (Supplementary Fig. 1), and were synthesized and cloned in the pUC57 vector (pUC57-3CL) by a custom gene synthesis service (GenScript, Piscataway, NJ, USA). The $3CL^{pro}$ gene was isolated from the vector pUC57-3CL by cutting with *Eco*RI and *Not*I, and was subcloned into the *Eco*RI/*Not*I restriction sites of the expression vector pPICZαA. The novel construct was named pPICZαA-$3CL^{pro}$ and transformed into *E. coli* DH5α (Promega, Madison, WI, USA) using a standard heat shock method. Transformants harbouring pPICZαA-$3CL^{pro}$ were selected from LB agar low salt medium [1% (w/v) Tryptone, 0.5% (w/v) yeast extract, 0.5% NaCl, pH 7.5] containing 25 μg Zeocin ml^{-1} (Invitrogen). Plasmid pPICZαA-$3CL^{pro}$ was amplified in *E. coli* DH5α, linearized by *Sac*I digestion, and transformed into *P. pastoris* GS115 by a modified LiCl method. pPICZαA vector was also linearized by *SacI* digestion and transformed into *P. pastoris* GS115 as a negative control strain. Screening for positive clones was done by PCR with two sets of primers (Bioneer, Deajeon, Korea): set one contained $3CL^{pro}$ primers [3CL-F (5′-GTGGATTCAGAAAAATGGCC-3′) and 3CL-R (5′-CCGCCTGAAAAGTAACTCCT-3′)] and set two contained α-factor and 3AOX1 primers. The PCR conditions were 94°C for 5 min, followed by 25 cycles of 94°C for 1 min, 53°C for 30 s, 72°C for 1 min, and a final step of 72°C for 5 min. PCR was conducted using PCRmix and the PCR product was analyzed by agarose gel electrophoresis.

Recombinant $3CL^{pro}$ was expressed according to the manufacturer's instructions (Invitrogen). Large-scale expression of $3CL^{pro}$ was carried out in a 10 l fermenter with 4 l BMMY medium. The fermentation conditions were 28°C, pH 6.0, 350 rpm, and aeration at 1 vvm. Methanol was added as described above.

Protein expression by pPICZαA transformed into *P. pastoris* GS115 was included as a negative control. The yeast was separated from the broth by centrifugation at 8,000×*g* for 15 min. The pellet was discarded and the supernatant was exchanged by 20 mM Tris/HCl buffer (pH 7.5) using a Millipore membrane. The supernatant was used for ammonium sulphate fractionation (from 0 to 85%). The obtained proteins were dissolved in 20 mM Tris/HCl buffer (pH 7.5) and dialyzed against 20 mM Tris/HCl buffer (pH 7.5). The detection of recombinant $3CL^{pro}$ in the culture supernatant was by 12% SDS-PAGE and western blot of the electrotransferred proteins according to to the manufacturer's instructions (GE Healthcare, Buckinghamshire, UK). Activity of the recombinant enzyme was detected as described below.

The proteolytic activity of $3CL^{pro}$ was measured using a fluorescence resonance energy transfer (FRET)-based assay with a substrate labeled with 5-[(2′-aminoethyl)-amino]naphthelenesulfonic acid (Edans) and 4-[{4-(dimehtylamino)phenyl}azo]benzoic acid (Dabcyl) as the energy transfer pair (Bachem, Bubendorf, Switzerland). The Dabcyl-KTSAVLQSGFRKME-Edans fluorogenic peptide was used as the substrate and the enhanced fluorescence due to cleavage of this substrate catalyzed by the protease was monitored at 538 nm with an excitation wavelength of 355 nm using a fluorescence plate reader. The reaction mixture contained 3 μg $3CL^{pro}$ protease and 20 μM fluorogenic substrate in 20 mM Tris/HCl buffer (pH 7.5) (Grum-Tokars et al. 2008). The plates were analyzed at 25°C with continuous monitoring of fluorescence for 25 min, with recording of relative fluorescence units (RFUs) using a SpectraMax Gemini XPS apparatus (Molecular Devices, Sunnyvale, CA, USA) with excitation and fluorescence emission wavelengths of 355 and 538 nm, respectively. Kinetic parameters of recombinant $3CL^{pro}$ were obtained using 12.5–100 μM FRET peptides in the fluorescent assay with an 18 min measurement period. Reaction responses were linear within this time. The (K_m) value was calculated from a Lineweaver–Burk using the SigmaPlot program (Systat Software, San Diego, CA, USA).

Inhibition assay

Quercetin, daidzein, puerarin, epigallocatechin (EGC), epigallocatechin gallate (EGCG), and gallocatechin gallate (GCG) were purchased from Sigma–Aldrich and ampelopsin (AMPLS) was purchased from ZR chemicals (Shanghai, China). Primarily inhibitory activities of flavonoid compounds were determined by measuring the remaining activity of $3CL^{pro}$ at 200 μM inhibitors. GCG, EGCG, and EGC were dissolved in water; quercetin, puerarin, daidzein, and AMPLS were dissolved in dimethylsulfoxide (DMSO) as 10 mM stock solutions. The enzyme reaction digest (100 μl) was composed of 3 μg enzyme, 20 μM FRET substrate, 200 μM of each flavonoid compound, and 20 mM Tris/HCl buffer (pH 7.5). Reactions were run for 18 min at 25°C with continuous monitoring of fluorescence. The inhibition was calculated using following formula (1): % inhibition = 100 − remaining activity (%) where the remaining activity (%) = $[(S - S_o)/(C - C_o)] \times 100$ (1), where C is the fluorescence of the control (enzyme, buffer, and substrate) after 18 min incubation, C_o is the fluorescence of the control at time zero, S is the fluorescence of the tested samples (enzyme, tested sample solution, buffer and substrate) after 18 min incubation, and S_o is the fluorescence of the tested samples at time zero. The 50% inhibitory concentration (IC_{50}) was defined as the concentration of $3CL^{pro}$ inhibitor necessary to reduce $3CL^{pro}$ activity by 50% relative to a reaction mixture containing $3CL^{pro}$ enzyme but no inhibitor. Inhibitor kinetic studies were performed for GCG, which was the best inhibitor against $3CL^{pro}$. The method was similar to those used in a kinetic study of the recombinant enzyme, except for the use of multiple concentrations of the inhibitor (0–60 μM) and variable concentrations of substrate (5–15 μM). The type of inhibition was determined using Lineweaver–Burk plots and a Dixon plot ($1/v$ as a function of inhibitor concentration, [I]) and kinetic parameters (K_i) was calculated using the SigmaPlot program.

Docking of flavonoid compounds with $3CL^{pro}$

The three-dimensional structure of $3CL^{pro}$ was retrieved from the Protein Data Bank [http://www.pdb.org, accession code 2ZU5]. *N*-[(benzyloxy)carbonyl]-*O*-tert-butyl-L-threonyl-*N*-[(1R)-4-cyclopropyl-4-oxo-1-{[(3S)-2-oxopyrrolidin-3-yl]methyl}butyl]-L-leucinamide (ZU5) was located in the active site of 2ZU5 (Lee et al. 2009). All water molecules, co-crystal ligand ZU5 were removed and the structure information containing only the amino acid residues of the $3CL^{pro}$ enzyme was used for

docking. Docking files were prepared using AutoDockTools software (Sanner et al. 1996). For the protein molecules, polar hydrogen atoms were added and nonpolar hydrogen atoms were merged. Kollman charges and solvation parameters were assigned by default. The three-dimensional atomic coordinates of GCG were generated by the Corina program (Molecular Networks GmbH, Erlangen, Germany), Gasteiger charges were added and nonpolar hydrogen atoms were merged. The grid box, with grid spacing of 0.375 Å and dimensions of $60 \times 60 \times 60$ points along the x, y, and z axes, was centered on the macromolecule. AutoDock version 3.0.5 software using the Lamarckian genetic algorithm (LGA) was used for the computational molecular docking simulation of flexible small molecules to rigid proteins with ligand and rigid proteins (Morris et al. 1998). Important docking parameters for the Lamarckian genetic algorithm were a population size of 250 individuals, maximum of 5 million energy evaluations, maximum of 27,000 generations, mutation rate of 0.02, crossover rate of 0.80, and 100 docking runs (each docking job produced 100 docked conformations). The probability of performing a local search on an individual in the population was set to 0.06 and the maximum number of iterations per local search was set to 300. The conformation with the lowest docked energy was chosen from the most populated cluster and was put through to the next stage. The hydrogen bond (H-bond) interaction between $3CL^{pro}$ and GCG was identified by Ligplot software (Wallace et al. 1995).

Results and discussion

Recombinant $3CL^{pro}$ enzyme preparation

The 918 bp gene encoding $3CL^{pro}$ (amino acids 3,241–3,546) from human SARS-CoV was cloned into the pPICZαA expression vector (pPICZαA-$3CL^{pro}$) and the pPICZαA-$3CL^{pro}$ plasmid was linearized by *Sac*I digestion that was further incorporated into the AOX1 locus of *Pichia pastoris*. Seven colonies were identified as $3CL^{pro}$-positive by PCR (Supplementary Fig 2). A single clone was selected for expression; the recombinant $3CL^{pro}$ was resolved electrophoretically as a band of approx. 42 kDa. To confirm that the clone secreted $3CL^{pro}$, western blotting was performed using the anti-His antibody; $3CL^{pro}$ was apparent as the same band upon SDS-PAGE and the control did not show this band on Western blot (Supplementary Fig 3).

Large-scale expression of $3CL^{pro}$ was carried out in a 10 l fermenter with 4 l BMMY medium. $3CL^{pro}$ was secreted and the amount of $3CL^{pro}$ protein was increased as the induction time increased (Fig. 1a) as confirmed by western blot analysis (Fig. 1b). After 4 days induction, the RFU (as representative of enzyme activity) was increased 2.4-times compared with 3 days induction. Electrophoretic analysis of the $3CL^{pro}$ fraction obtained using ammonium sulfate gave 80% purity (Supplementary Fig 4). The yields of each step in the procedure are summarized in Supplementary Table 1. No appreciable glycosylation was observed for $3CL^{pro}$ even after endoglycosidase H treatment.

To calculate the kinetic parameters of the purified $3CL^{pro}$, enzyme activity was analyzed with fluorescent substrate from 12.5 to 100 μM. The Km value was 15 ± 1 μM (Supplementary Fig 5). The K_m value of the purified $3CL^{pro}$ was similar to the K_m value of $3CL^{pro}$ expressed in *E. coli* (K_m of 17 ± 4 μM) (Kuo et al. 2004).

$3CL^{pro}$ inhibition by flavonoid compounds

Seven flavonoid compounds belonging to four groups of flavonoids (flavonol, flavanonol, isoflavone, and flavan-3-ol) (Fig. 2) were evaluated for their inhibitory activity against $3CL^{pro}$ expressed from *P. pastoris* GS115. Table 1 shows the inhibitory activity of each flavonoid against the $3CL^{pro}$ at 200 μM. Quercetin, EGCG and GCG inhibited more than 80% of the activity of recombinant $3CL^{pro}$; AMPLS, puerarin, and daidzein inhibited more than 30% activity of recombinant $3CL^{pro}$; and EGC inhibited only 5% of the activity of recombinant $3CL^{pro}$. Six compounds displayed an IC_{50} ranging from 47 to 381 μM (Table 1). GCG showed the best inhibition against recombinant $3CL^{pro}$ with IC_{50} value of 47 ± 0.9 μM, and so was used for the further analysis of inhibition mode. Both Lineweaver–Burk and Dixon plots were used. As shown in Fig. 3a, GCG exhibited competitive inhibition toward $3CL^{pro}$ because the Lineweaver–Burk plot of $1/v$ versus $1/[S]$ resulted in a family of straight lines with the same y-axis intercept. The K_i value of GCG was determined to be 25 ± 1.7 μM

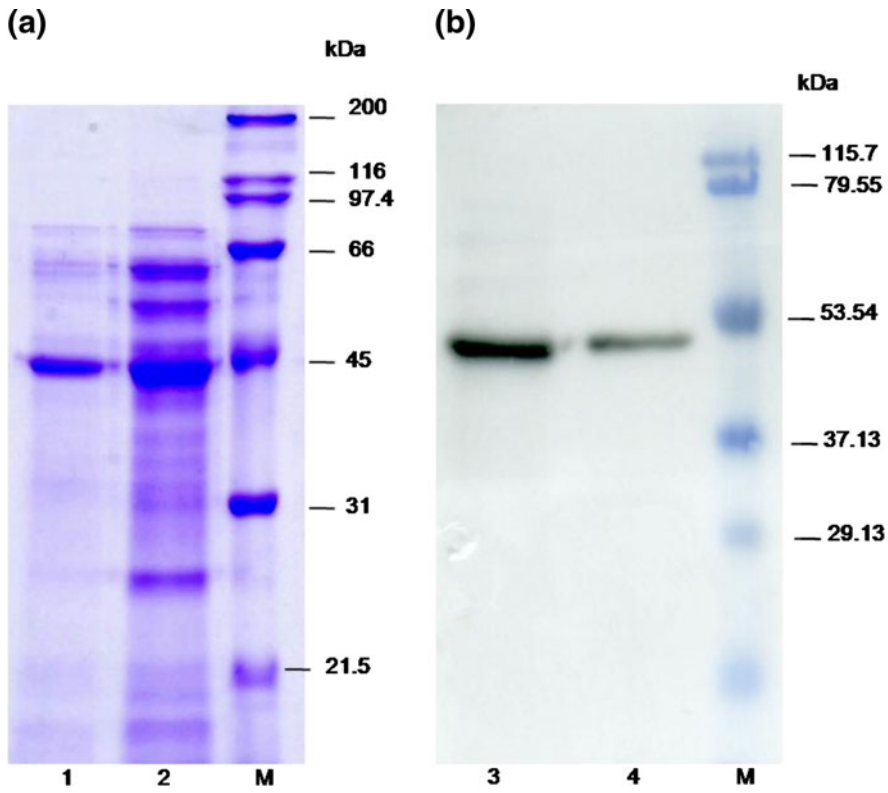

Fig. 1 SDS-PAGE and Western blot results of recombinant $3CL^{pro}$ after 3 and 4 days induction during fermentor culture. *Lane M*: marker; *lanes 1* and *2*: SDS-PAGE after 3 days (*lane 1*) and 4 days (*lane 2*); *lanes 3* and *4*: Western blot conducted after 3 days (*lane 4*) and 4 days (*lane 3*)

from the common *x*-axis intercept of lines on the corresponding Dixon plot (Fig. 3b).

Molecular docking on $3CL^{pro}$

In order to get a better comprehension of the molecular recognition process between $3CL^{pro}$ and antioxidant compounds, docking experiments were performed using the crystal structure of $3CL^{pro}$ (2ZU5). Autodock 3.0.5 was used to carry out docking simulations. The free binding energy of flavonoid compounds is shown in Table 1. Among them, GCG displayed the lowest free binding energy (-14 kcal mol^{-1}). The binding between GCG and active site pocket of $3CL^{pro}$ is shown in Fig. 4a. To elucidate the interaction of $3CL^{pro}$ with GCG, the potential hydrophobic and H-bond interactions between amino acid residues in the active site pockets of 3CLpro and GCG were investigated using the Ligplot program. Figure 4b depicts the details of the specific interactions between GCG and $3CL^{pro}$. Carbon atoms of GCG interacted hydrophobically with His41, Cys145, Met165, Glu166, Asp187, Arg188, and Gln189 of $3CL^{pro}$. GCG formed seven hydrogen bonds with residues in the catalytic binding pocket of $3CL^{pro}$. The O atom of the main chain carboxyl group of Glu166 formed an H-bond with the O^{33} atom of the 5-hydroxyl group of the A ring with a distance of 2.56 Å. The O atom of hydroxyl group of aromatic side chain of Tyr54 formed a H-bond with the O^{30} atom of the 4′-hydroxyl group of the ring B at 2.7 Å. The O^{29} atom of the 5′-hydroxyl group of ring B accepted a H-bond from the N atom of the imidazol group of His41with a distance 2.72 Å. The O^{28} atom of the 3″-hydroxyl group of the galloyl group accepted a H-bond with the N atom from the imidazol group of His163 with a distance of 2.96 Å. The O^{26} atom of the 4″-hydroxyl group of the galloyl group has two H-bonds: one with the carboxyl group of Leu141 and another one with the carboxyl group of Ser144 at 2.90 and 2.49 Å, respectively. The N atom of the amino group of Gly143 donated a H-bond with an O^{27} atom of the 5″-hydroxyl group of the galloyl group with a distance of 3.35 Å.

Structural activity relationships of flavonoid compounds

In this study, we compared the inhibition activity of AMPLS, EGC, EGCG, and GCG containing the same

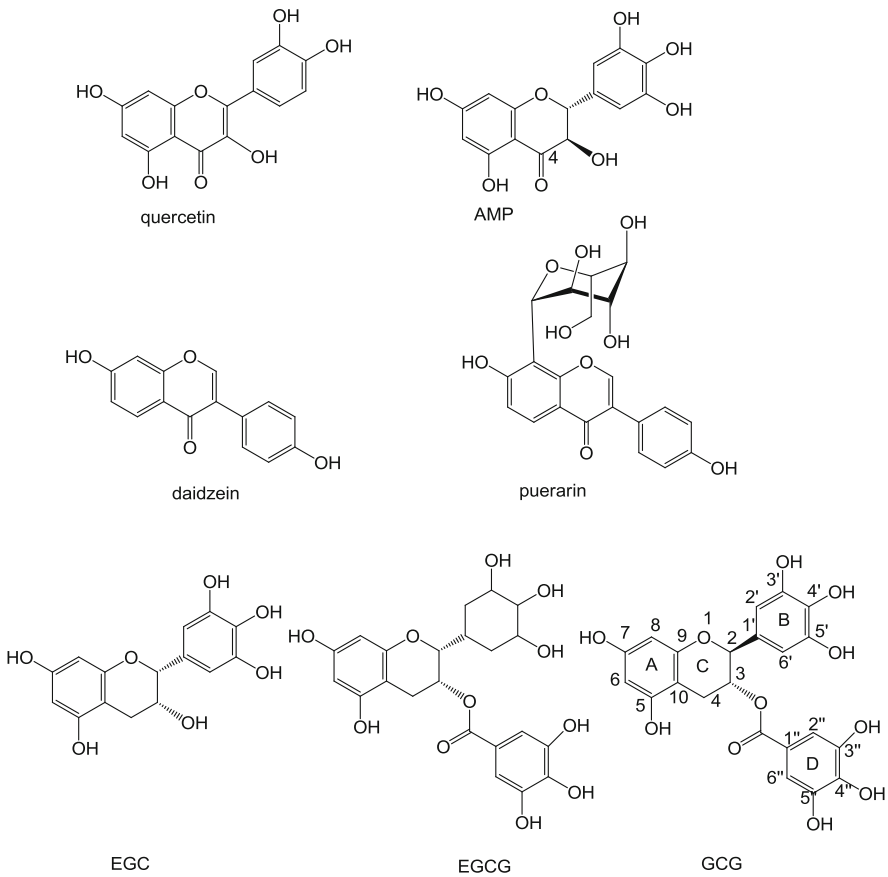

Fig. 2 Molecular structures of the seven flavonoids

Table 1 Inhibitory activity of flavonoid compounds against $3CL^{pro}$

Compound	Inhibition[a] (%)	IC_{50} (μM)	Docking score (kcal mol^{-1})
AMPLS	34	364 ± 8.7	−9.9
Quercetin	82	73 ± 4	−10.2
Puerarin	33	381 ± 12.5	−11.3
Daidzein	34	351 ± 2.9	−8.6
EGC	5.4	ND	−9.3
EGCG	85	73 ± 2	−11.7
GCG	91	47 ± 0.9	−14.1

ND not determined, *GCG* gallocatechin gallate, *EGCG* epigallocatechin gallate, *EGC* epigallocatechin, *AMPLS* ampelopsin

[a] Inhibition by 200 μM

B-ring at 200 μM (Table 1). The decreasing order of the inhibitory activity was EGC < AMPLS < EGCG < GCG. EGCG and GCG have a galloyl moiety at the 3-OH position, which is absent in the other catechins used in this study. EGCG and GCG displayed stronger $3CL^{pro}$ inhibitory activity than those of EGC and AMPLS. GCG (2S, 3R type), which is a C-2 epimeric isomer of EGCG (2R, 3R type), showed 1.5-times higher $3CL^{pro}$ inhibitory activity than that of EGCG. Molecular docking simulation was used to calculate the binding of GCG to the $3CL^{pro}$ active site. GCG bound at the substrate-binding pocket of $3CL^{pro}$ with numerous hydrophobic and hydrogen bond interactions. The galloyl group from GCG was important for GCG binding to $3CL^{pro}$ active site pocket because it has four hydrogen bond interactions with Leu141, Gly143, Ser144, and His163 (Fig. 4b). The effect of B-ring and hydroxyl group substitution on the B-ring for the inhibitory activity was evaluated. Daidzein and puerarin, which lack the B-ring, showed little inhibition of $3CL^{pro}$. The $3CL^{pro}$ inhibitory activity of AMLSP was 4.96-times lower than that of quercetin. This confirmed that the addition of an OH group at 5′-position of the B ring decreased the $3CL^{pro}$ inhibitory activity. The effect of the structures of the A and C rings on the inhibitory activity was evaluated. Since AMPLS, which lacks the 2,3-double bonds in

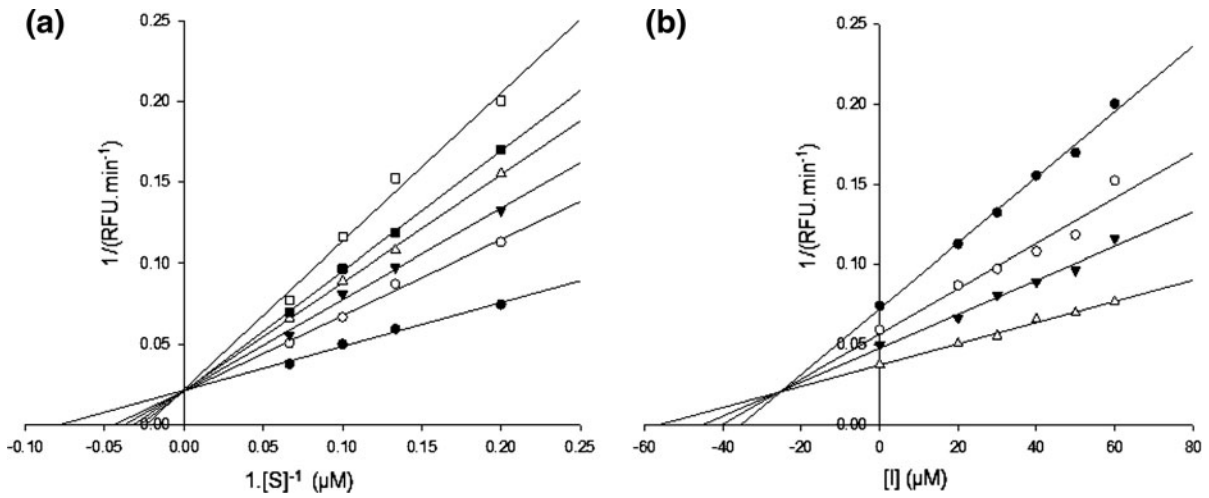

Fig. 3 Lineweaver-Burk plot (**a**) and Dixon plot (**b**) analyses for the inhibition of $3CL^{pro}$ by GCG. The kinetic constants, K_m and K_i, were calculated using linear regression analysis. **a** GCG concentration 0 μM (*filled circle*), 20 μM (*open circle*), 30 μM (*filled inverted triangle*), 40 μM (*open triangle*), 50 μM (*filled square*), 60 μM (*open square*). **b** FRET substrate concentrations 5 μM (*filled circle*), 7.5 μM (*open circle*), 10 μM (*filled inverted triangle*), and 15 μM (*triangle*)

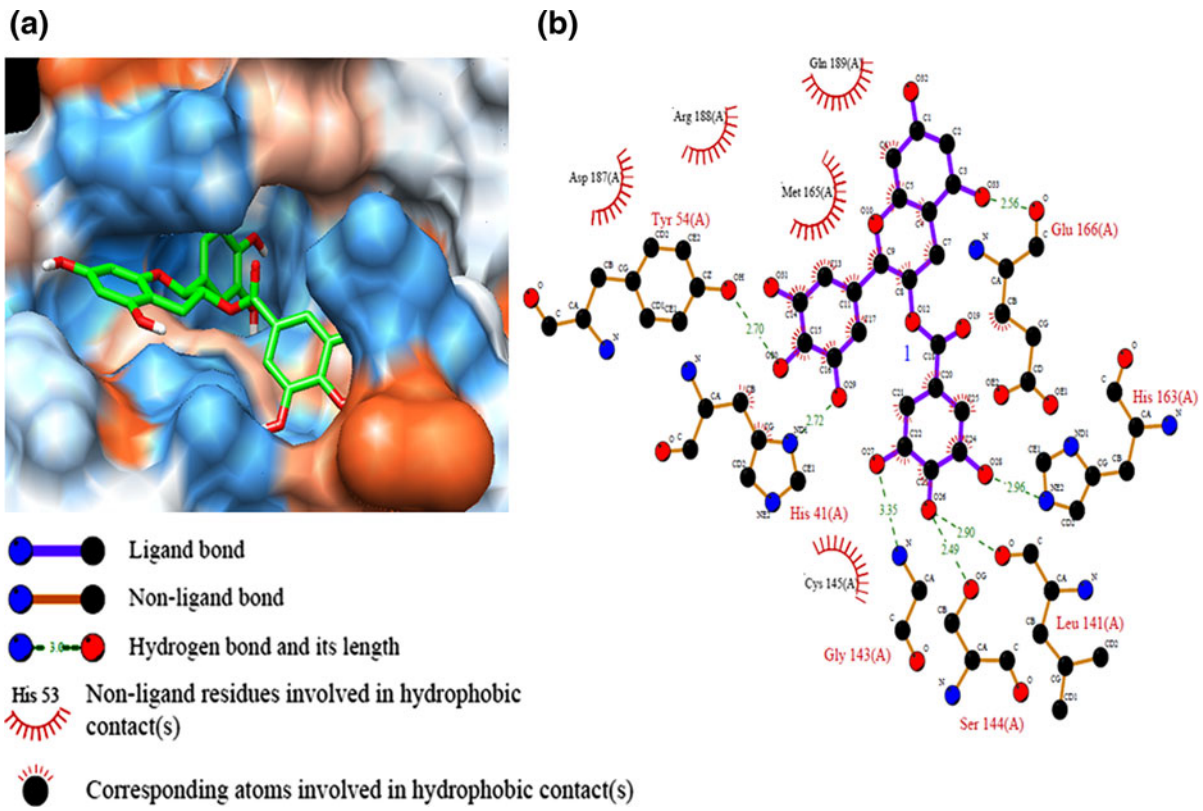

Fig. 4 Computational docking and hydrophobic and hydrogen bond interactions of GCG with amino acid residues in the active site of $3CL^{pro}$. **a** Comparison of binding modes of GCG (*green*) in the active site pocket of $3CL^{pro}$. **b** Hydrophobic and H-bond interactions between GCG and amino acid residues in the active site of $3CL^{pro}$. H-bond interactions are represented by *green dashed lines* (*Red*, oxygen; cornflower *blue*, nitrogen; *black*, carbon)

the C-ring, showed lower inhibitory activity than that of quercetin, 2,3-double bonds are probably crucially influential to the inhibitory activity. EGC lacking the C(4)=O in the C-ring, C(2)=C(3), containing 5′-OH group and lacking galloyl moiety showed the lowest inhibitory activity compared to that of AMPLS, daidzein, puerarin, quercetin, EGCG, or GCG.

Conclusions

An important goal of the present study was to understand the inhibition by seven flavonoid compounds belonging to four groups of flavonoids (flavonol, flavanonol, isoflavone, and flavan-3-ol) against $3CL^{pro}$ of SARS-CoV. The active extracellular $3CL^{pro}$ was successfully expressed and purified in *P. pastoris* GS115. Among the investigated flavonoids, GCG was the best inhibitor against $3CL^{pro}$ by an in vitro assay. The structure and inhibition activity relationship among seven flavonoid compounds was also investigated. GCG showed numerous hydrophobic and H-bonds interaction with amino acid residues in the active site pocket of $3CL^{pro}$.

Acknowledgments This work was partially supported by 21C Frontier Microbial Genomics and the Applications Center Program.

References

Benson DA, Karsch-Mizrachi I, Lipman DJ, Ostell J, Sayers EW (2011) GenBank. Nucleic Acids Res 39:D32–D37

Chen CN, Lin CPC, Huang KK, Chen WC, Hsieh HP, Liang PH, Hsu JTA (2005) Inhibition of SARS-CoV 3C-like protease activity by theaflavin-3, 3′-digallate (TF3). Evid Based Compliment Altern Med 2:209–215

Chen L, Li J, Luo C, Liu H, Xu W, Chen G, Liew OW, Zhu W, Puah CM, Shen X, Jiang H (2006) Binding interaction of quercetin-3-beta-galactoside and its synthetic derivatives with SARS-CoV 3CL(pro): structure–activity relationship studies reveal salient pharmacophore features. Bioorg Med Chem 14:8295–8306

de Groot H, Rauen U (1998) Tissue injury by reactive oxygen species and the protective effects of flavonoids. Fund Clin Pharmacol 12(3):249–255

Grum-Tokars V, Ratia K, Begaye A, Baker SC, Mesecar AD (2008) Evaluating the 3C-like protease activity of SARS-Coronavirus: recommendations for standardized assays for drug discovery. Virus Res 133:63–73

Kuo CJ, Chi YH, Hsu JT, Liang PH (2004) Characterization of SARS main protease and inhibitor assay using a fluorogenic substrate. Biochem Biophys Res Commun 318:862–867

Lee CC, Kuo CJ, Ko TP, Hsu MF, Tsui YC, Chang SC, Yang S, Chen SJ, Chen HC, Hsu MC, Shih SR, Liang PH, Wang AHJ (2009) Structural basis of inhibition specificities of 3C and 3C-like proteases by zinc-coordinating and peptidomimetic compounds. J Biol Chem 284:7646–7655

Morris GM, Goodsell DS, Halliday RS, Huey R, Hart WE, Belew RK, Olson AJ (1998) Automated docking using a Lamarckian genetic algorithm and an empirical binding free energy function. J Comput Chem 19:1639–1662

Rota PA, Oberste MS, Monroe SS et al (2003) Characterization of a novel coronavirus associated with severe acute respiratory syndrome. Science 300:1394–1399

Sanner MF, Olson AJ, Spehner JC (1996) Reduced surface: an efficient way to compute molecular surfaces. Biopolymers 38:305–320

Tadera K, Minami Y, Takamatsu K, Matsuoka T (2006) Inhibition of alpha-glucosidase and alpha-amylase by flavonoids. J Nutr Sci Vitam 52:149–153

Tapas AR, Sakarkar DM, Kakde RB (2008) Flavonoids as nutraceuticals: a review. Trop J Pharm Res 7:1089–1099

Wallace AC, Laskowski RA, Thornton JM (1995) Ligplot—a program to generate schematic diagrams of protein ligand interactions. Protein Eng 8:127–134

Xu T, Ooi A, Lee HC, Wilmouth R, Liu DX, Lescar J (2005) Structure of the SARS coronavirus main proteinase as an active C-2 crystallographic dimer. Acta Crystallogr F 61:964–966

Yi L, Li Z, Yuan K et al (2004) Small molecules blocking the entry of severe acute respiratory syndrome coronavirus into host cells. J Virol 78:11334–11339